[7] Q. Y. Chen, S. W. Qu, X. Q. Zhang, and M. Y. Xia, "Low-profile wideband reflectarray by novel elements with linear phase response," *IEEE Antennas Wireless Propag. Lett.*, vol. 11, pp. 1545–1547, 2012.
[8] Q.-Y. Chen, S.-W. Qu, J.-F. Li, Q. Chen, and M.-Y. Xia, "An X-band reflectarray with novel elements and enhanced bandwidth," *IEEE Antennas Wireless Propag. Lett.*, vol. 12, pp. 317–320, 2013.
[9] E. Carrasco, M. Barba, and J. A. Encinar, "Reflectarray element based on aperture-coupled patches with slots and lines of variable length," *IEEE Trans. Antennas Propag.*, vol. 55, no. 3, pp. 820–825, Mar. 2007.
[10] Y. Mao, S. Xu, F. Yang, and A. Z. Elsherbeni, "A novel phase synthesis approach for wideband reflectarray design," *IEEE Trans. Antennas Propag.*, vol. 63, no. 9, pp. 4189–4193, Sep. 2015.
[11] D. M. Pozar, "Wideband reflectarrays using artificial impedance surfaces," *Electron. Lett.*, vol. 43, no. 3, pp. 148–149, Feb. 2007.
[12] P. Nayeri, F. Yang, and A. Z. Elsherbeni, "Bandwidth improvement of reflectarray antennas using closely spaced elements," *Prog. Electromagn. Res. C*, vol. 18, pp. 19–29, 2011.
[13] J. Ethier, M. R. Chaharmir, and J. Shaker, "Reflectarray design comprised of sub-wavelength coupled-resonant square loop elements," *Electron. Lett.*, vol. 47, no. 22, pp. 1215–1217, Oct. 2011.
[14] P. Nayeri, F. Yang, and A. Z. Elsherbeni, "Broadband reflectarray antennas using double-layer subwavelength patch elements," *IEEE Antennas Wireless Propag. Lett.*, vol. 9, pp. 1139–1142, 2010.
[15] L. Guo, P.-K. Tan, and T.-H. Chio, "Bandwidth improvement of reflectarrays using single-layered double concentric circular ring elements on a subwavelength grid," *Microw. Opt. Technol. Lett.*, vol. 56, no. 2, pp. 418–421, Feb. 2014.
[16] J. A. Encinar, "Design of a dual frequency reflectarray using microstrip stacked patches of variable size," *Electron. Lett.*, vol. 32, no. 12, pp. 1049–1050, Jun. 1996.
[17] M. R. Chaharmir, J. Shaker, N. Gagnon, and D. Lee, "Design of broadband, single layer dual-band large reflectarray using multi open loop elements," *IEEE Trans. Antennas Propagat.*, vol. 58, no. 9, pp. 2875–2883, Sep. 2010.
[18] C. Han, C. Rodenbeck, J. Huang, and K. Chang, "A C/Ka dual frequency dual layer circularly polarized reflectarray antenna with microstrip ring elements," *IEEE Trans. Antennas Propag.*, vol. 52, no. 11, pp. 2871–2876, Nov. 2004.
[19] J. A. Encinar, M. Arrebola, L. de la Fuente, and G. Toso, "A transmit-receive reflectarray antenna for direct broadcast satellite applications," *IEEE Trans. Antennas Propag.*, vol. 59, no. 9, pp. 3255–3264, Sep. 2011.
[20] M. R. Chaharmir, J. Shaker, and H. Legay, "Dual-band Ka/X reflectarray with broadband loop elements," *IET Microw. Antennas Propag.*, vol. 4, no. 2, pp. 225–231, 2010.
[21] S.-W. Qu, Q.-Y. Chen, M.-Y. Xia, and X. YinZhang, "Single-layer dual-band reflectarray with single linear polarization," *IEEE Trans. Antennas Propag.*, vol. 62, no. 1, pp. 199–205, Jan. 2014.
[22] R. S. Malfajani and Z. Atlasbaf, "Design and implementation of a dual-band single layer reflectarray in X and K bands," *IEEE Trans. Antennas Propag.*, vol. 62, no. 8, pp. 4425–4431, Aug. 2014.
[23] J. A. Encinar and M. Barba, "Design manufacture and test of Ka-band reflectarray antenna for trasmitting and receiving in orthogonal polarization," in *Proc. 14th Int. Symp. Antenna Technol. Appl. Electromagn. Amer. Electromagn. Conf. (ANTEM-AMEREM)*, Ottawa, ON, Canada, 2010, pp. 1–4.
[24] J. A. Encinar *et al.*, "Dual-polarization dual-coverage reflectarray for space applications," *IEEE Trans. Antennas Propag.*, vol. 54, no. 10, pp. 2827–2837, Oct. 2006.
[25] S. D. Targonski and D. M. Pozar, "Analysis and design of a microstrip reflectarray using patches of variable size," *Antennas Propag. Soc. Int. Symp. Dig.*, Seattle, WA, USA, Jun. 1994, pp. 1820–1823.
[26] A. Yu, F. Yang, A. Z. Elsherbeni, J. Huang, and Y. Rahmat-Samii, "Aperture efficiency analysis of reflectarray antennas," *Microw. Opt. Technol. Lett.*, vol. 52, no. 2, pp. 364–372, Feb. 2010.

Single End-Fire Antenna for Dual-Beam and Broad Beamwidth Operation at 60 GHz by Artificially Modifying the Permittivity of the Antenna Substrate

Abdolmehdi Dadgarpour, Behnam Zarghooni, Bal S. Virdee, and Tayeb A. Denidni

***Abstract*— A technique is proposed to generate a dual-beam and broad beamwidth radiation in the *E*-plane of a printed bow-tie antenna operating over 57–64 GHz. This is achieved by artificially modifying the dielectric constant of the antenna substrate using arrays of metamaterial inclusions realized using stub-loaded H-shaped unit cells to provide a high index of refraction. The H-shaped inclusions are tilted with respect to the axis of the antenna and embedded in the direction of the end-fire radiation. The resulting dual-beam radiation in the *E*-plane has maxima at +60° and 120° with respect to the end-fire direction (90°), with a maximum peak gain of 9 dBi at 60 GHz.**

***Index Terms*— 5G wireless networks, antenna, bow-tie antenna, broad beamwidth, dual-beam, millimeter-wave antennas.**

I. Introduction

Recently, the work at millimeter-wave frequency band, in particular at 60 GHz, has attracted the attention of researchers as this band offers transmission rates of multigigabits per second, which is necessary for applications requiring video streaming and Internet-of-things/machine-to-machine communications to be implemented in 5G wireless networks [1], [2].

Working at this frequency band is particularly challenging because the quality of the communication link is degraded by: 1) substantial loss due to atmospheric absorption; 2) interference effect from adjacent channels; 3) multipath effect causing signal fading; and 4) link blockage by obstructions. The loss can be compensated using high-gain antennas. In order to overcome the interference effect and where coverage of multiple nonadjacent areas is required, it is necessary to employ multibeam antennas. Such antennas confine the power in specific directions instead of scattering the power everywhere. In [3], improved spatial diversity is demonstrated with dual-beam Multiple Input Multiple Output (MIMO) compared with the classical MIMO, where a power gain of 1.6 dB is achieved at the 60 GHz band. Hosoya *et al.* [4] and Ma *et al.* [5] have shown that employing a dual-beam antenna at the transmitter and receiver improves the link quality where the

Manuscript received September 28, 2015; revised April 11, 2016; accepted May 17, 2016. Date of publication June 1, 2016; date of current version September 1, 2016.

A. Dadgarpour was with the Institut National de la Recherche Scientifique-Énergie Matériaux Télécommunications, University of Quebec, Montreal, QC H5A 1K6, Canada. He is now with the Department of Electrical and Computer Engineering, Concordia University, Montreal, QC H3G 1M8, Canada (e-mail: mehdidadgar60@gmail.com).

B. Zarghooni is with the Poly-Grames Research Center, École Polytechnique de Montréal, Montreal, QC H3T 1J4, Canada (e-mail: behnam.zarghooni@polymtl.ca).

B. S. Virdee is with the Center for Communications Technology, London Metropolitan University, London N7 8DB, U.K. (e-mail: b.virdee@londonmet.ac.uk).

T. A. Denidni is with the Institut National de la Recherche Scientifique-Énergie Matériaux Télécommunications, University of Quebec, Montreal, QC H5A 1K6, Canada (e-mail: denidni@emt.inrs.ca).

Color versions of one or more of the figures in this communication are available online at http://ieeexplore.ieee.org.

Digital Object Identifier 10.1109/TAP.2016.2574881

link blockage is encountered due to multipath effect and mutual interference. Dual-beam antennas that radiate energy symmetrically at two different angles also find application in scanning and millimeter-wave identification (MMID) systems [6]–[8]. Various types of antennas with different functionalities have been studied at millimeter-wave frequencies.

For instance, end-fire radiating antennas, such as Yagi-Uda, dipole, as well as bow-tie, have been widely reported for millimeter-wave frequency band applications, in particular, beam switching networks, beam tilting, and beam steering [9]–[16].

One approach to generate multiple beams or dual beams is to employ antenna arrays with an adaptive radiation pattern using phased array antennas [17]. To implement this technique requires multiple antenna arrays as well as phase shifters, which makes this approach costly and requiring a larger footprint size. To overcome these limitations, Dadgarpour *et al.* [18] have utilized gradient index of refraction media in the classical dipole antenna. By switching the appropriate feed line in the antenna structure, the direction of the main beam can be steered toward one of two specific angles. To achieve multiple beams with this technique requires electronically controlled single-pole double-throw switches that can introduce extra loss and complexity into the system.

Pattern reconfigurability is another promising technique reported in [19], where Electromagnetic bandgap structures are placed symmetrically around the 60 GHz antenna to achieve beam steering by means of switching diodes ON or OFF. Although the radiation pattern of the antenna can be steered at discrete angles in the azimuth plane the diodes introduce extra loss and complexity into the system.

Extensive investigation has been carried out to obtain the dual-beam radiation pattern using leaky-wave antennas [20]–[24]. The drawback of these antennas is the dual-beam radiation pattern is affected by the frequency, which restricts its applications. To overcome this limitation, Khidre *et al.* [25] have excited a higher TM_{02} mode in a U-slot patch antenna to realize a dual-beam with a wide beamwidth. Although the radiation beam is fixed over the antenna's operating frequency range of 5.18–5.8 GHz, the antenna gain is relatively low for practical applications.

In this communication, a technique is proposed to realize a dual-beam antenna for millimeter-wave applications over 57–64 GHz. This is realized on an end-fire bow-tie antenna by incorporating metamaterial inclusions that are implemented with stub-loaded H-shaped unit cells. The array of 4×4 inclusions are tilted with respect to the end-fire direction. Reduction in the back-lobe radiation and enhancement of the antenna gain is achieved by loading a pair of H-shaped resonators next to the feed line near the bow-tie radiators. To improve the coverage of the communications link over the designated area it is necessary to widen the beamwidth of the antenna, which is particularly challenging at the 60 GHz band [26]. We have broadened the 3-dB beamwidth of the antenna by including an array of nontilted 2×3 inclusions in the end-fire direction of the bow-tie radiators. The measured reflection coefficient of the antenna is better than -10 dB over 57–64 GHz and the two radiation beams generated point at angles of 60° and 120° with respect to the end-fire direction (90°) with a maximum peak realized gain of 9 dBi. These properties make such an antenna suitable for improving the communications link of systems affected by multipath effect and mutual interference [4], [5], and in scanning and MMID applications [6]–[8]. In [18], we have employed gradient index of refraction with multiple dipole antennas with switches to generate dual-beam radiation, where the beam deflection is limited to angles $+26°$ and $-26°$. By exciting individual antennas separately using SP4T switches, we are able to generate dual-beam radiation that is limited to angles $+26°$ and $-26°$ with respect to the end-fire direction.

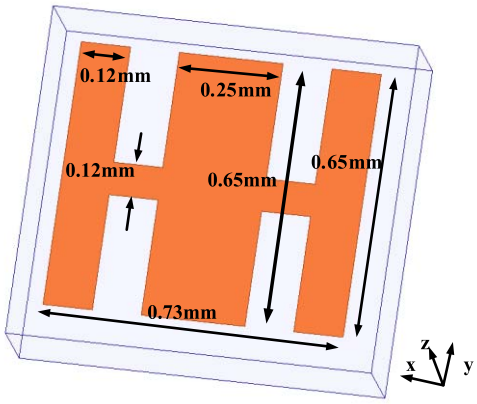

Fig. 1. Geometry of the proposed H-shaped metamaterial unit cell fabricated on the dielectric substrate (RO5880).

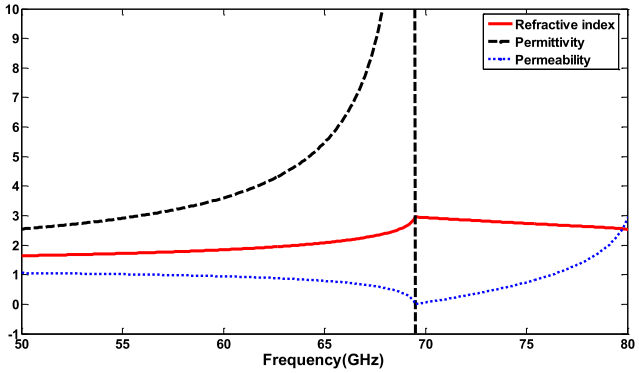

Fig. 2. Extracted characterizing parameters of proposed unit cell including real part of permittivity and permeability as well as refractive index.

However, as can be observed in [18, Fig. 18] we are unable to achieve dual-beam when both feeds are excited simultaneously, in which case a single main beam is created that radiates in the end-fire direction.

II. Mechanism of Dual-Beam

Here, dual-beam radiation is established by exploiting the dielectric slab mode TE in the printed bow-tie dipole antenna as described in [27] and [28]. To excite TE surface modes, it is necessary to utilize high dielectric constant substrates [29]. It is well known that a high dielectric constant substrate can adversely affect the antenna's radiation efficiency and gain performance as the electromagnetic energy is confined within the substrate. Hence, the bow-tie antenna used here was designed on a low dielectric constant substrate (RO5880) with a relative dielectric constant of 2.2.

When excited, the printed bow-tie antenna launches TE surface waves and the resulting radiation emanating from the antenna is tailored to point toward a predefined angle by creating a region of high refractive index on the antenna. This was achieved by embedding metamaterial unit-cell inclusions described in [18]. Integration of metamaterial inclusions on the RO5880 substrate was designed to artificially increase the effective dielectric constant of the substrate in order to refract the electromagnetic radiation from the bow-tie antenna. This technique was implemented here using an array of stub-loaded H-shaped electric resonators or unit cells as shown in Fig. 1.

The unit cell's intrinsic parameters were extracted using HFSS software tools by locating the perfect electric conductor and perfect magnetic conductor boundary conditions in the *yz* and *xy* planes with the two wave ports arranged along the *y*-direction [30]. Hence, when the electric-field is polarized in the optical

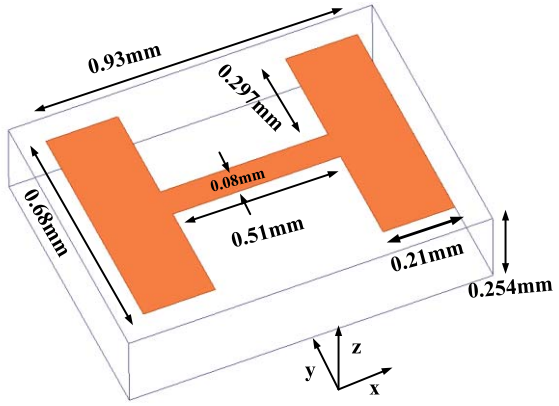

Fig. 3. Structure of the H-shaped unit cell.

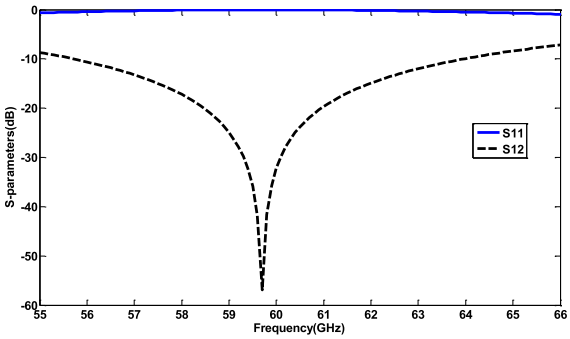

Fig. 4. S-parameter (S_{12} and S_{11}) response of the H-shaped configuration.

axis of the proposed unit cell in the x-direction, the electric resonance is generated and the proposed unit cell can be regarded as an LC resonator. Fig. 2 shows that the real part of permittivity varies from 3.2 to 7.3 over the frequency range of 57–64 GHz. The operational region of the unit cell needs to be far away from its resonant frequency to minimize the loss. The corresponding refractive index varies from 1.81 to 2.22, which is larger than the antenna substrate with an effective refractive-index value of 1.28. Hence, embedding the proposed unit cells in front of end-fire radiation will cause the antenna to excite surface waves whose phase velocity is lower than the phase velocity of the waves in the substrate, thus altering the direction of the radiation.

In order to improve the gain of the antenna and reduce its back-lobe radiation, a pair of H-shaped resonators, shown in Fig. 3, was loaded onto the antenna. The S-parameter response of the resonator was obtained by exciting the two wave ports in the y-direction in order to induce electric and magnetic fields in the x- and z-direction, respectively. The transmission coefficient response of the proposed structure in Fig. 4 indicates that it has a band-stop response over 57–64 GHz. In Section III, it is shown that by integrating the proposed H-shaped resonators at the back side of the end-fire antenna results in the suppression of backward surface waves that are reflected at the edge of the ground plane [16].

III. Dual-Beam Radiation Pattern in the Azimuth Plane

The proposed antenna, shown in Fig. 5, comprises printed bow-tie radiators constructed on Rogers 5880 substrate with a relative dielectric constant 2.2 and thickness 0.254 mm. The bow-tie radiators are fed by microstrip lines that are tapered at its end to improve its impedance match. The antenna is loaded with two H-shaped resonators next to the feed line and just below the bow-tie radiators

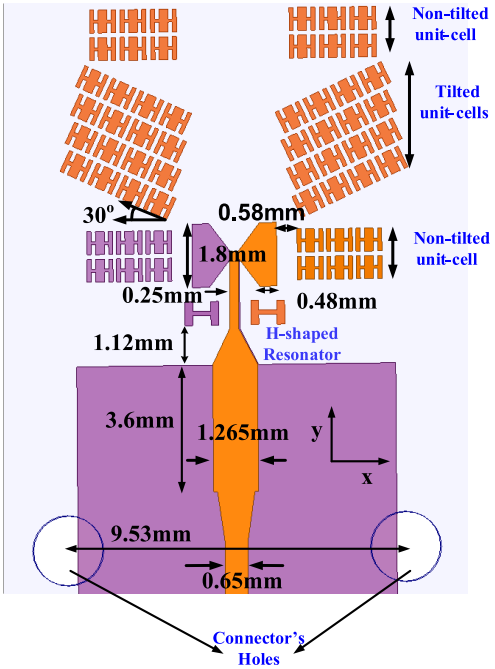

Fig. 5. Configuration of the antenna embedded with a 3 × 4 array of the proposed HRIM unit cells on the upper surface of the antenna substrate.

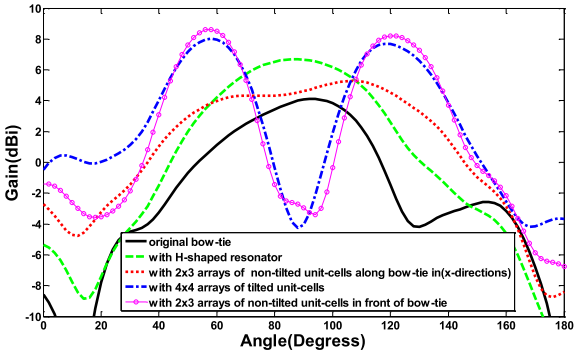

Fig. 6. Radiation pattern of antenna in the E-plane with different arrangements of tilted and nontilted unit cells at 60 GHz.

to minimize the back-lobe and side radiation. Fig. 6 shows that these unit cells effectively enhance the antenna gain by 2.66 dB from 4.1 to 6.76 dBi.

Embedded in the antenna are arrays of nontilted stub-loaded H-shaped unit cells placed along the x-direction of the bow-tie antenna, as shown in Fig. 5, whose purpose is to broaden the beamwidth. It can be observed in Fig. 6 that loading the antenna with nontilted unit cells contributes to increasing the 3-dB beamwidth of the bow-tie antenna by 67° from 53° to 120° compared with the conventional bow-tie antenna with a 3-dB beamwidth of 53° (62°–115°). This property can be used for providing a broader coverage for wireless communications over 57–64 GHz. This means that we have a radiation at 53° and 120° with respect to the end-fire direction (90°) compared with the conventional bow-tie antenna as shown in Fig. 6. Thus, we can generate a dual-beam radiation by embedding onto the antenna, unit cells that are tilted by 30° with respect to the antenna's axis. The reason that we have tilted the proposed unit cells by 30° is attributed to the increase in the 3-dB beamwidth of the antenna by 67/2 = 33° in each direction with respect to the antenna's axis. Thus, we can obtain a larger steer angle by simply increasing the 3-dB beamwidth to more than 67°.

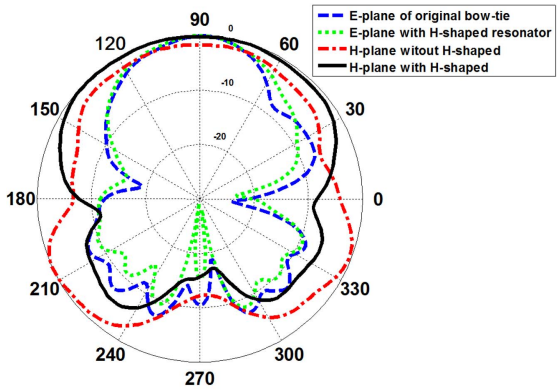

Fig. 7. E- and H-plane radiation patterns of the bow-tie antenna with and without H-shaped resonators.

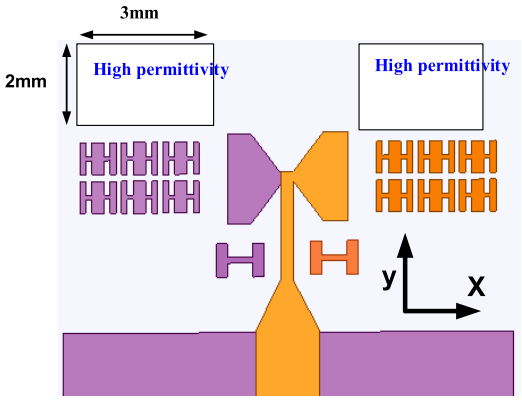

Fig. 8. Configuration of the bow-tie antenna embedded with high dielectric constant material instead of stub-loaded H-shaped unit cells.

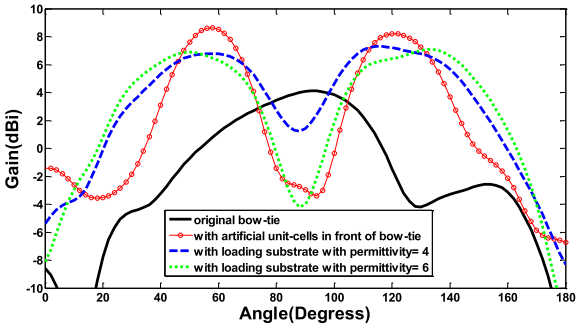

Fig. 9. Radiation patterns of the antenna in the E-plane when loaded with higher dielectric constant substrates.

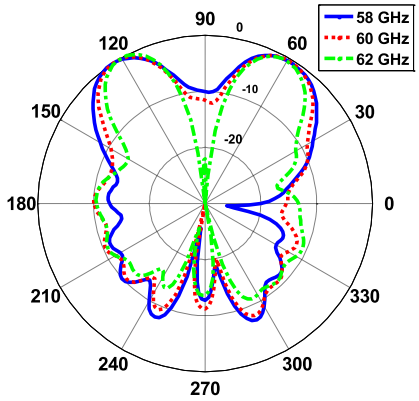

Fig. 10. Normalized radiation patterns of the dual-beam bow-tie antenna in the E-plane (xy) at 58, 60, and 62 GHz.

As mentioned in Section II, in order to excite TE surface waves, it is necessary to integrate a higher refractive index medium in the end-fire region of the bow-tie antenna. This is achieved here by artificially creating a higher index of refraction using an array of stub-loaded H-shaped unit cells that exhibit a higher effective permittivity and refractive index than the antenna substrate, as is evident in Fig. 2. In particular, the 4×4 arrays of stub-loaded H-shaped unit cells were integrated in the end-fire direction (y-axis) of the bow-tie radiators, as shown in Fig. 5. The 4×4 arrays are tilted by 30° with respect to the end-fire direction. The result of this arrangement, shown in Fig. 6, reveals that at 60 GHz the dual-beam radiation pattern is created with a maximum peak gain of 7.9 dBi at 60° and 120° with respect to end-fire radiation (90°). Introducing another 2×3 array of nontilted stub-loaded H-shaped unit cells in front of the tilted unit cells enhances the antenna gain by 1 dBi. Furthermore, the 2×3 array reduces the side-lobe level by almost 4 dB.

To better exemplify the effect of H-shaped inclusions on the antenna, the radiation pattern of the original bow-tie antenna with and without H-shaped resonators is plotted in Fig. 7. It can be observed that by embedding the H-shaped resonators on the back side of the bow-tie antenna results in the improvement in back-lobe radiation by about 5 dB in the H-plane. This leads to gain enhancement in the end-fire direction compared with the original bow-tie, as shown in Fig. 6.

The TE mode surface waves were excited by artificially creating a high dielectric constant region in the end-fire vicinity of the bow-tie antenna by embedding arrays of stub-loaded H-shaped unit cells. To validate the approach undertaken, high dielectric constant substrates with permittivity of 4 and 6 were integrated into the antenna substrate, as shown in Fig. 8. The antenna substrate had a permittivity of 2.2. The result of this study in Fig. 9 shows that when a substrate with dielectric constant 4 was used, the antenna exhibits dual-beam radiation in the azimuth plane at 60° and 120° with a maximum gain of about 7 dBi, which is analogous to loading the antenna with artificial metamaterial inclusions. When a substrate with dielectric constant 6 is used, the antenna radiates dual-beam at 50° and 130° with a maximum gain of 7 dBi. Although the maximum angle of the radiation beam with a loaded substrate is the same as for artificial inclusions, the antenna gain with stub-loaded H-shaped unit cells is higher by 3 dB.

The dual-beam radiation pattern in the E-plane of the final antenna design at 58, 60, and 62 GHz is plotted in Fig. 10. It is evident that at the three different frequencies, the antenna exhibits a maximum radiation at $+60°$ and 120°. Also, the radiation null in the end-fire direction improves significantly from -10 to -30 dBi with increase in the frequency from 58 to 62 GHz. The worst case null of -10 dBi at 58 GHz is sufficient for applications such as scanning and MMID systems, as only a tenth of the power is radiated in the undesired direction. The 3-dB beamwidth of the antenna tends to decrease from 32° at 58 GHz to 23° at 62 GHz. The measured gain corresponding to 58, 60, and 63 GHz is 8.7, 8.9, and 9.2 dBi, respectively. This variation is tolerable for 60-GHz band systems.

The size of the tilted unit-cell array was obtained from a parametric study. Increasing the number of unit cells in the x-direction from 2×4 to 4×4 attenuates spurious radiation directed toward the end-fire (90°) by 24 dB, as shown in Fig. 11. Increasing the number of unit cells from 2×4 to 4×4 in the y-axis results in attenuation of the end-fire radiation by 20 dB.

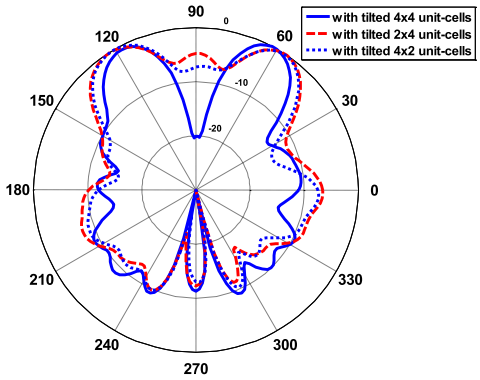

Fig. 11. Normalized radiation patterns of the dual-beam bow-tie antenna in the E-plane (xy) obtained by loading different number of tilted unit cells along the x- and y-directions at 60 GHz.

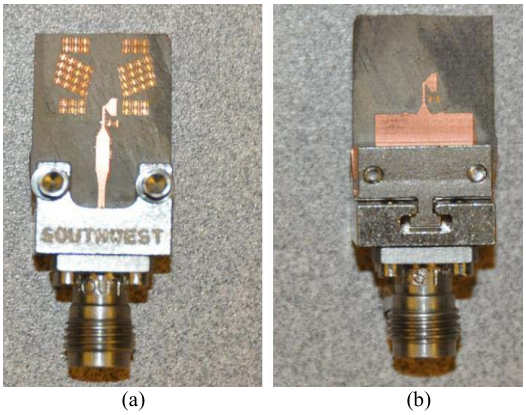

(a) (b)

Fig. 12. Photograph of the dual-beam bow-tie antenna loaded with stub-loaded H-shaped unit cells, (a) Top view, (b) bottom view.

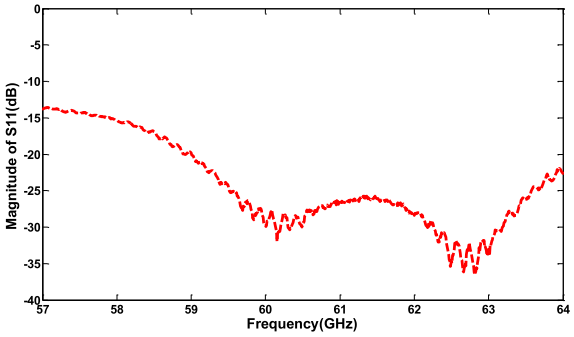

Fig. 13. Measured reflection coefficient of the dual-beam bow-tie antenna.

IV. Experimental Results

A photograph of the fabricated dual-beam bow-tie antenna with arrays of stub-loaded H-shaped unit cells is shown in Fig. 12. The proposed antenna was constructed on a Rogers RT5880. A 1.85-mm end-launch Southwest Connector was utilized in the measurement of the antenna characteristics. The measured reflection coefficient of the proposed bow-tie antenna is shown in Fig. 13. The magnitude of S_{11} is better than -10 dB over the frequency band of 55–65 GHz.

It is important to emphasize that the work presented here can be regarded as a quasi-Yagi antenna, and fabrication of this antenna is not complicated as the metamaterial unit cells can be easily etched in the plane of the antenna using conventional MIC technology. We have used standard manufacturing facilities available to us at the university.

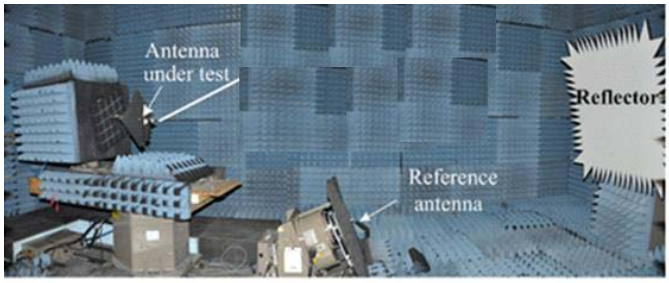

Fig. 14. Equipment setup to measure the radiation patterns and gain of the proposed antenna.

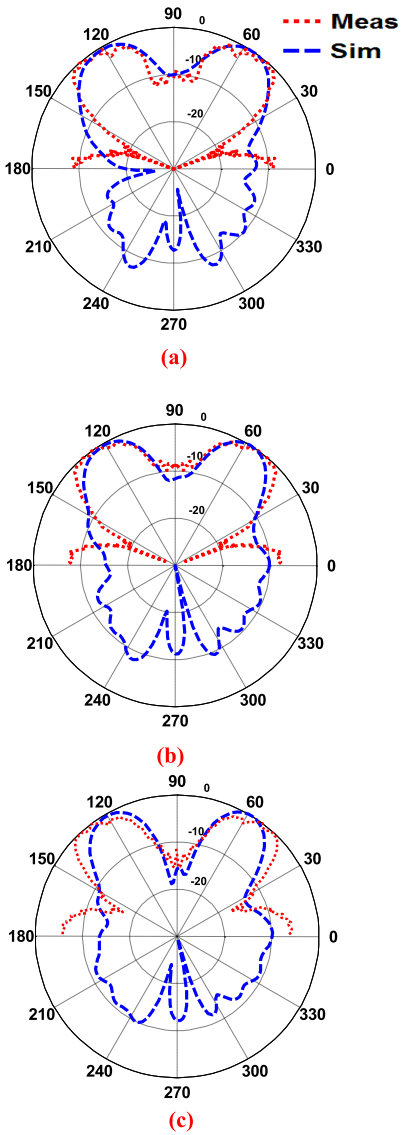

Fig. 15. Normalized radiation patterns of the dual-beam bow-tie antenna using an array of stub-loaded H-shaped unit cells in the E-plane (xy) at (a) 58, (b) 60, and (c) 63 GHz.

Antenna gain was measured using a compact range anechoic chamber, as shown in Fig. 14, where the reference horn antenna is located at the focal point of the reflector that converts spherical waves to plane waves directed to the antenna under test. The antenna gain was measured using the comparison method as explained in [16],

by measuring the power received by the reference horn antenna and the proposed dual-beam bow-tie antenna, and determining the relative difference in the gain of both the antennas. In addition, the connector losses were taken into account according to [16]. There is good agreement between the simulation and measured results shown in Fig. 15.

The simulated and measured E-plane radiation pattern of the bow-tie antenna at 58, 60, and 63 GHz are shown in Fig. 15. The measured results show that the main beam direction of the antenna radiates at $+60°$ and $120°$ with respect to the end-fire direction (90°). In addition, the magnitude of the normalized E-plane radiation in the end-fire direction corresponds to -10 and -15 dBi at 58 and 63 GHz, respectively. The discrepancy between the simulation and measured results is attributed to the fabrication tolerance.

The measured antenna gain at 58, 60, and 63 GHz are 8.7, 8.9, and 9.2 dBi, respectively. The proposed antenna is applicable for millimeter-wave indoor communication systems.

V. Conclusion

It has been demonstrated that by artificially manipulating the dielectric constant of the substrate in the end-fire direction of a bow-tie antenna, a dual-beam radiation pattern can be realized in the E-plane at 60 GHz. This is achieved using 4×4 arrays of metamaterial inclusions implemented using stub-loaded H-shaped unit cells. By appropriately tilting the inclusions with respect to the bow-tie axis, a dual-beam was created at $+60°$ and $120°$. In addition, it was shown that by including a pair of H-shape resonators in the vicinity of the feed line and the radiators, the back-lobe radiation is reduced and the antenna gain is enhanced by 2.66 dB. Inclusion of a further 2×3 array of metamaterial inclusions was used to broaden the 3-dB beamwidth of the antenna and enhance its gain by 1 dB. The measured results of the prototype antenna agree well with the simulation results. This antenna exhibits desirable characteristics for indoor communications at 60 GHz.

References

[1] K.-H. Li, M. A. Ingram, and E. O. Rausch, "Multibeam antennas for indoor wireless communications," *IEEE Trans. Commun.*, vol. 50, no. 2, pp. 192–194, Feb. 2002.

[2] O. Elloumi, J. Song, Y. Ghamri-Doudane, and V. C. M. Leung, "IoT/M2M from research to standards: The next steps (part I) [Guest Editorial]," *IEEE Commun. Mag.*, vol. 53, no. 9, pp. 8–9, Sep. 2015.

[3] S. Kirthiga and M. Jayakumar, "Performance of dualbeam MIMO for millimeter wave indoor communication systems," *Wireless Pers. Commun.*, vol. 77, no. 1, pp. 289–307, 2014.

[4] K. Hosoya *et al.*, "Multiple sector ID capture (MIDC): A novel beamforming technique for 60-GHz band multi-Gbps WLAN/PAN systems," *IEEE Trans. Antennas Propag.*, vol. 81, no. 1, pp. 81–96, Jan. 2015.

[5] Z. L. Ma, C. H. Chan, K. B. Ng, and L. J. Jiang, "A supercell based dual beam dielectric grating antenna for 60 GHz application," in *Proc. IEEE Int. Symp. Antennas Propag., USNC/URSI Nat. Radio Sci. Meeting*, Jul. 2015, pp. 643–644.

[6] A. Lamminen, J. Aurinsalo, J. Säily, T. Karttaavi, J. Francey, and T. Bateman, "Dual-circular polarised patch antenna array on LCP for 60 GHz millimetre-wave identification," in *Proc. Eur. Conf. Antennas Propag. (EuCAP)*, Apr. 2014, pp. 537–541.

[7] M.-Y. Li, C. T. Rodenbeck, and K. Chang, "Millimeter-wave dual-beam scanning microstrip patch antenna arrays fed by dielectric image lines," in *Proc. IEEE Antennas Propag. Soc. Int. Symp.*, vol. 2. 2002, pp. 196–199.

[8] S. Raman and G. M. Rebeiz, "Single- and dual-polarized millimeter-wave slot-ring antennas," *IEEE Trans. Antennas Propag.*, vol. 44, no. 11, pp. 1438–1444, Nov. 1996.

[9] R. A. Alhalabi, Y.-C. Chiou, and G. M. Rebeiz, "Self-shielded high-efficiency Yagi–Uda antennas for 60 GHz communications," *IEEE Trans. Antennas Propag.*, vol. 59, no. 3, pp. 742–750, Mar. 2011.

[10] S. Jafarlou, M. Bakri-Kassem, M. Fakharzadeh, Z. Sotoodeh, and S. Safavi-Naeini, "A wideband CPW-fed planar dielectric tapered antenna with parasitic elements for 60-GHz integrated application," *IEEE Trans. Antennas Propag.*, vol. 62, no. 12, pp. 6010–6018, Dec. 2014.

[11] R. A. Alhalabi and G. M. Rebeiz, "High-gain Yagi–Uda antennas for millimeter-wave switched-beam systems," *IEEE Trans. Antennas Propag.*, vol. 57, no. 11, pp. 3672–3676, Nov. 2009.

[12] M. Sun, Z. N. Chen, and X. Qing, "Gain enhancement of 60-GHz antipodal tapered slot antenna using zero-index metamaterial," *IEEE Trans. Antennas Propag.*, vol. 61, no. 4, pp. 1741–1746, Apr. 2013.

[13] A. Dadgarpour, B. Zarghooni, B. S. Virdee, and T. A. Denidni, "Beam tilting antenna using integrated metamaterial loading," *IEEE Trans. Antennas Propag.*, vol. 62, no. 5, pp. 2874–2879, May 2014.

[14] A. Dadgarpour, B. Zarghooni, B. S. Virdee, and T. A. Denidni, "Improvement of gain and elevation tilt angle using metamaterial loading for millimeter-wave applications," *IEEE Antennas Wireless Propag. Lett.*, vol. 15, pp. 418–420, 2016.

[15] B. Zarghooni, A. Dadgarpour, and T. A. Denidni, "Millimeter-wave antenna using two-sectioned metamaterial medium," *IEEE Antennas Wireless Propag. Lett.*, vol. 15, pp. 960–963, 2016.

[16] A. Dadgarpour, B. Zarghooni, B. S. Virdee, and T. A. Denidni, "Millimeter-wave high-gain SIW end-fire bow-tie antenna," *IEEE Trans. Antennas Propag.*, vol. 63, no. 5, pp. 2337–2342, May 2015.

[17] S.-G. Kim and K. Chang, "Independently controllable dual-feed dual-beam phased array using piezoelectric transducers," *IEEE Antennas Wireless Propag. Lett.*, vol. 1, no. 1, pp. 81–83, 2002.

[18] A. Dadgarpour, B. Zarghooni, B. S. Virdee, and T. A. Denidni, "Beam-deflection using gradient refractive-index media for 60-GHz end-fire antenna," *IEEE Trans. Antennas Propag.*, vol. 63, no. 8, pp. 3768–3774, Aug. 2015.

[19] M. Al-Hasan, T. Denidni, and A. R. Sebak, "60 GHz agile EBG-based antenna with reconfigurable pattern," in *Proc. IEEE Int. Symp. Antennas Propag., USNC/URSI Nat. Radio Sci. Meeting*, Jul. 2015, pp. 13–14.

[20] A. Mehdipour, J. W. Wong, and G. V. Eleftheriades, "Beam-squinting reduction of leaky-wave antennas using huygens metasurfaces," *IEEE Trans. Antennas Propag.*, vol. 63, no. 3, pp. 978–992, Mar. 2015.

[21] W. Cao, W. Hong, Z. N. Chen, B. Zhang, and A. Liu, "Gain enhancement of beam scanning substrate integrated waveguide slot array antennas using a phase-correcting grating cover," *IEEE Trans. Antennas Propag.*, vol. 62, no. 9, pp. 4584–4591, Sep. 2014.

[22] T.-L. Chen and Y.-D. Lin, "Dual-beam microstrip leaky-wave array excited by aperture-coupling method," *IEEE Trans. Antennas Propag.*, vol. 51, no. 9, pp. 2496–2498, Sep. 2003.

[23] Z. L. Ma and L. J. Jiang, "One-dimensional triple periodic dual-beam microstrip leaky-wave antenna," *IEEE Antennas Wireless Propag. Lett.*, vol. 14, pp. 390–393, 2015.

[24] C.-C. Hu, C. F. Jsu, and J.-J. Wu, "An aperture-coupled linear microstrip leaky-wave antenna array with two-dimensional dual-beam scanning capability," *IEEE Trans. Antennas Propag.*, vol. 48, no. 6, pp. 909–913, Jun. 2000.

[25] A. Khidre, K. F. Lee, A. Z. Elsherbeni, and F. Yang, "Wide band dual-beam U-slot microstrip antenna," *IEEE Trans. Antennas Propag.*, vol. 61, no. 3, pp. 1415–1418, Mar. 2013.

[26] M. Sun, X. Qing, and Z. N. Chen, "60-GHz end-fire fan-like antennas with wide beamwidth," *IEEE Trans. Antennas Propag.*, vol. 61, no. 4, pp. 1616–1622, Apr. 2013.

[27] A. L. Amadjikpe, D. Choudhury, C. E. Patterson, B. Lacroix, G. E. Ponchak, and J. Papapolymerou, "Integrated 60-GHz antenna on multilayer organic package with broadside and end-fire radiation," *IEEE Trans. Microw. Theory Techn.*, vol. 61, no. 1, pp. 303–315, Jan. 2013.

[28] K. M. K. H. Leong, Y. Qian, and T. Itoh, "Surface wave enhanced broadband planar antenna for wireless applications," *IEEE Microw. Wireless Compon. Lett.*, vol. 11, no. 2, pp. 62–64, Feb. 2001.

[29] N. G. Alexopoulos, P. B. Katehi, and D. B. Rutledge, "Substrate optimization for integrated circuit antennas," *IEEE Trans. Microw. Theory Techn.*, vol. 31, no. 7, pp. 550–557, Jul. 1983.

[30] Z. Szabó, G.-H. Park, R. Hedge, and E.-P. Li, "A unique extraction of metamaterial parameters based on Kramers–Kronig relationship," *IEEE Trans. Microw. Theory Techn.*, vol. 58, no. 10, pp. 2646–2653, Oct. 2010.